

DOI:10.19948/j.12-1471/P.2024.03.02

何胜飞,刘晓阳,孙凯,许康康,龚鹏辉. 2024. 坦桑尼亚卢帕地体花岗岩岩石地球化学特征、锆石U-Pb年代学及其构造意义[J]. 华北地质, 47(3):14-22+35.

He Shengfei, Liu Xiaoyang, Sun Kai, Xu Kangkang, Gong Penghui. 2024. Geochemical characteristics, Zircon U-Pb isotopic and the indicative geotectonic environment of the granitoids in Lupa terrain, Tanzania[J]. North China Geology, 47(3):14-22+35.

坦桑尼亚卢帕地体花岗岩岩石地球化学特征、 锆石U-Pb年代学及其构造意义

何胜飞^{1,2},刘晓阳^{1,2},孙凯^{1,2},许康康^{1,2},龚鹏辉^{1,2}

(1.中国地质调查局天津地质调查中心(华北地质科技创新中心),天津300170;

2.中国地质调查局南部非洲矿业研究所,天津300170)

摘要:【研究目的】卢帕地体是坦桑尼亚第二大金矿集区所在地,对于其形成时代及成因机制争议较大。【研究方法】本次通过锆石年代学和地球化学特征分析,厘定卢帕地体花岗岩的形成时代和成因机制。【研究结果】锆石U-Pb年代学研究表明卢帕地体内花岗岩有两类:新太古代花岗岩类,年龄为 $2\ 663 \pm 22\text{ Ma} \sim 2\ 778 \pm 13\text{ Ma}$;古元古代花岗岩年龄为 $1\ 944 \pm 10\text{ Ma} \sim 2\ 006 \pm 10\text{ Ma}$,地球化学特征与I型花岗岩相似。卢帕地体内分布的其它基性岩、碳酸岩等代表了罗迪尼亞超大陆裂解开始的时间。【结论】岩石地球化学特征表明非A型花岗岩,其物质来源并非来自地幔,而是地壳重熔的结果。花岗岩构造环境判别图解显示,样品投影落在火山弧花岗岩中,花岗岩集中于大陆花岗岩区域,远离大洋花岗岩、大洋玄武岩和辉长岩区域,新太古代与古元古代的花岗岩形成于大陆边缘弧。

关键词:锆石U-Pb年代学;地球化学特征;卢帕地体;坦桑尼亚

创新点:通过锆石U-Pb年代学、岩石地球化学特征研究,确定卢帕地体花岗岩形成于古元古代,是地壳重融的结果,构造环境归属于大陆边缘弧。

中图分类号:P548; P581 文献标志码:A 文章编号:2097-0188(2024)03-0014-10

Geochemical characteristics, Zircon U-Pb isotopic and the indicative geotectonic environment of the granitoids in Lupa terrain, Tanzania

HE Shengfei^{1,2}, LIU Xiaoyang^{1,2}, SUN Kai^{1,2}, XU Kangkang^{1,2}, GONG Penghui^{1,2}

(1. Tianjin Centre, China Geological Survey (North China Center for Geoscience Innovation), Tianjin 300170, China;

2. Southern African Mining Research Institute, China Geological Survey, Tianjin 300170, China)

Abstract: This paper is the result of rock geochemistry.

[Objective] Lupa terrane is the second largest gold ore concentration area in Tanzania, and its formation age and genetic mechanism

收稿日期:2023-09-18

基金项目:中国地质调查项目“非洲中东部7国矿产资源潜力评价项目(DD20160108)”;“非洲中东部大型铜钴资源基地评价(DD20190439)”;“南部非洲国际合作地质调查(DD20221801, DD20230125)”

作者简介:何胜飞(1977-),男,硕士,高级工程师,主要从事中南部非洲基础地质调查研究工作,E-mail:hesan496112@163.com。

are controversy. [Methods] Through the analysis of zircon geochronology and geochemical characteristics of granite, the formation age and genetic mechanism of the Lupa terrane granite are determined. [Results] Zircon U-Pb geochronology studies indicate that there are two types of granites in the Lupa terrane: Neoarchean granites ($2\ 663 \pm 22$ Ma ~ $2\ 778 \pm 13$ Ma); Paleoproterozoic granite ($1\ 944 \pm 10$ Ma ~ $2\ 006 \pm 10$ Ma), and their geochemical characteristics are similar to those of I-type granite. The other basic rocks, carbonates and other rocks distributed within the earth represent the beginning of the breakup of the Rodinian super continent. [Conclusions] The geochemical characteristics of rocks indicate that the material source of non-A-type granite is not from the mantle, but the result of crustal remelting. The tectonic environment discrimination diagram of the granite shows that the sample projection falls in the volcanic arc granite, and the granite is concentrated in the continental granite area, away from the oceanic granite, oceanic basalt and gabbro area. The Neoarchean and Paleoproterozoic granites were formed in the continental margin arc.

Key words: Zircon U-Pb geochronology; geochemical characteristics; Lupa terrane; Tanzania

Highlights: Through the study of zircon U-Pb chronology and rock geochemical characteristics, it is determined that the granite of Lupa terrane was formed in Paleoproterozoic, which is the result of crustal remelting, and the tectonic environment belongs to the continental margin arc.

About the first author: He Shengfei, male, born in 1977, senior engineer, engaged in geological and mineral research in Central and Southern Africa, E-mail : hesan496112@163.com.

Fund Support: Supported by the projects of China Geological Survey (No.DD20160108); (No.DD20190439); (No.DD20221801, No.DD20230125)

卢帕地体(Lupa terrane)或卢帕金矿田(Lupa Goldfield)紧邻坦桑尼亚克拉通(Tanzanian Craton)西南缘(图1,图2),是NW-SE向古元古代乌本迪活动带(Ubendian mobile belt)的次级地质单元(Daly et al., 1985; Daly, 1988; Lenoir et al., 1994; Lawly et al., 2013a, 2013b; 吴兴源等, 2018; 许康康等, 2019; 刘晓阳等, 2019; 何胜飞等, 2021; 龚鹏辉, 2023)。卢帕金矿田是坦桑尼亚第二大金矿集区,仅次于维多利亚湖南岸金矿集区(王杰等, 2022)。

鲁夸断裂(Rukwa Fault)或卢帕断层(Lupa Fault)是坦桑尼亚克拉通与元古代乌本迪活动带的界限(Guest, 1954),而位于鲁夸湖(Lake Rukwa)西北的卢帕地体被认为是坦桑尼亚克拉通的一部分,萨扎(Saza)至马孔格罗西(Makongolosi, Ma)获得的新太古代花岗岩的年龄数据也从侧面支撑了这一结论(Manya 2011; Lawly et al., 2014)。然而,卢帕地体内大规模分布的伊伦加(Ilunga)花岗岩的年龄(Manya 2011, 2012; Lawly et al., 2013a, 2013b)、基性岩(Manya, 2012; Kazimoto, et al., 2014; 许康康等, 2021)、以及其北部的Ngualla碳酸岩(Tulibonywa et al., 2015)的形成年龄均为元古代,暗示其并非坦桑尼亚克拉通的组成部分。花岗岩的Nd同位素

模式年龄数据(T_{DM})甚至将坦桑尼亚克拉通太古宙与元古代的界限北推至距离卢帕断层约120 km的伦瓜镇(Rungwa, Ru)南3 km处(Manya, 2011),因此将卢帕地体形成时代划为元古宙。这说明卢帕地体成因复杂,其物质来源与形成的构造环境(Manya, 2011; Lawly et al., 2014)有待商榷,查明该地区岩浆岩的物质来源将有利于开展卢帕金矿田中金矿的勘探与增储。本文拟利用前人资料(Manya, 2011, 2012a, 2012b; Kazimoto, 2014; Lawly et al., 2014, 许康康等, 2020, 2021)和本文实验测试结果综合分析卢帕地体中不同时代花岗岩的锆石年代学特征和全岩主微量元素地球化学特征,探讨其岩浆起源和构造环境。

1 地质背景

1.1 古元古代乌本迪活动带

古元古代乌本迪活动带呈NW-SE向展布于坦桑尼亚西南部,北东侧为坦桑尼亚克拉通,南西侧为班韦卢地块(Bangweulu Block),出露岩石岩性以黑云母石榴子石片麻岩为主,和少量的基性、超基性侵入岩,花岗闪长岩、闪长岩侵入体,角闪辉石片麻岩,富石英石榴子石辉石片麻岩,花岗岩、铁质石

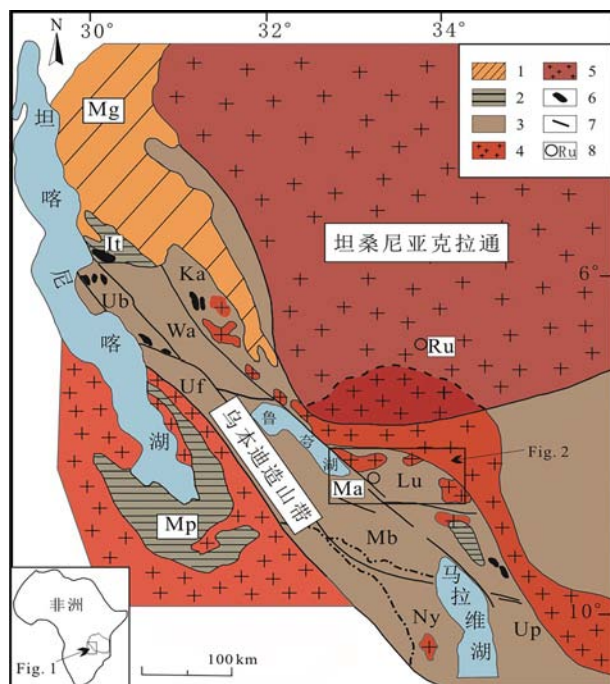


图1 坦桑尼亚乌本迪带地质简图及构造单元划分
(Lenoir et al., 1994; 有修改)

Fig.1 The geological sketch of Ubendian meta-mobile belt and its subdivision, Tanzania
(modified from Lenoir et al., 1994)

- 1.新元古宙马拉嘎拉西沉积岩；2.古元古代姆波洛科索群；
- 3.古元古代乌本迪变质活动带；4.古元古代花岗岩类；5.太古宙TTG；6.基性岩；7.断裂带；8.城镇；Ub.乌本德地体；Wa.瓦卡莱地体；Ka.卡通马地体；Uf.乌菲帕地体；Mb.姆柏兹地体；Lu.卢帕地体；Up.乌帕古地体；Ny.尼卡地体

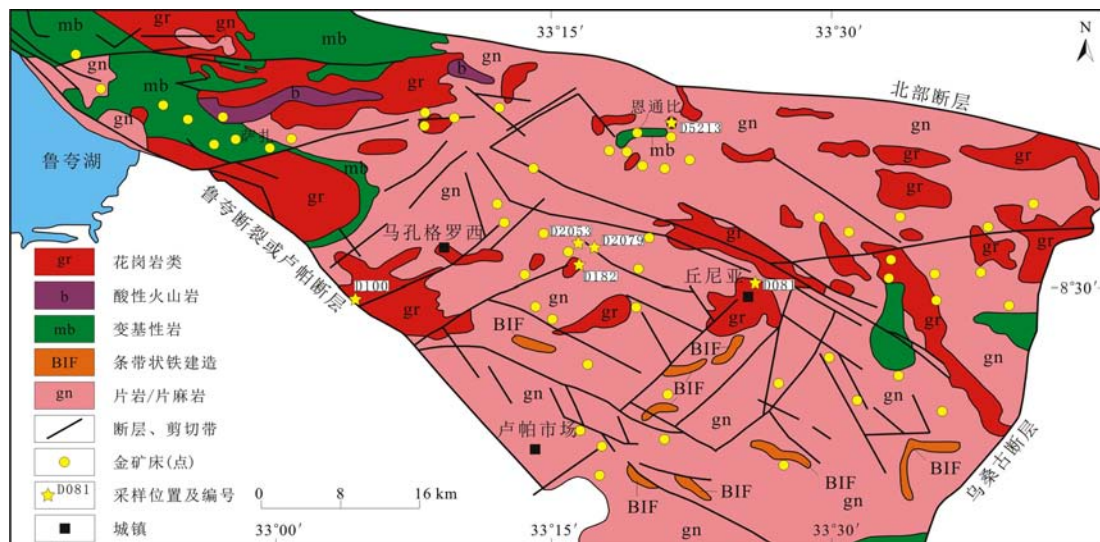


图2 坦桑尼亚卢帕地体地质简图(Lawley et al., 2013; Leger et al., 2015, 有修改)

Fig.2 The geological sketch map of Lupa Terrane, Tanzania
(modified from Lawley et al., 2013 and Leger et al., 2015)

英岩和云母片岩(Daly et al., 1985; Daly, 1988; Lenoir et al., 1994; Boniface and Schenk, 2012, 2014; Boniface et al., 2012; Tulibonywa, 2015)。乌本迪带在元古代经历了多次俯冲、地壳增长和钙碱性岩浆侵入作用(Boniface et al., 2012; Boniface and Schenk, 2012, 2014; Manya et al., 2014),最后一次大规模的区域性地质作用为约520 Ma的冈瓦纳大陆拼合事件(Boniface and Appel, 2018)。

1.2 卢帕地体

卢帕地体位于乌本迪活动带的东北,是一个紧邻坦桑尼亚克拉通的三角形块体(图2),三条边界分别为西南缘的鲁夸裂谷断裂带(Rukwa Rift Fault,或称卢帕断层),东南缘NE-SW向的乌桑古断层(Usangu Fault)和北部的北部断裂带(North Fault),总面积约3 000 km²,出露的岩石主要有辉长岩、花岗闪长岩、闪长岩、各种花岗岩体和变质火山岩等(Manya, 2011, 2012; Lawly et al., 2014; Kazimoto, 2014; Lawly et al., 2014; Leger et al., 2015; Tulibonywa, 2015; 许康康等,2020, 2021)。

2 采样与分析测试

采集、分析的样品均位于卢帕地体内,采样位置见图2。分析的样品共6件,均为花岗类岩石。

锆石的分离、挑选在河北廊坊宇能岩矿技术服务有限公司完成。锆石制靶、透射、反射和CL照相

均在北京锆年领航科技有限公司完成。简易流程是:采用浮选、磁选等方法分离,然后在双目镜下随机挑选锆石单矿物颗粒粘贴、浇铸于环树脂靶中,经打磨、抛光直至锆石核部出露,在显微镜下观察锆石颗粒结构、特征,圈定靶标。

主微量元素含量的实验分析工作和锆石U-Pb同位素测试分两次在中国地质调查局天津地质调查中心实验室完成。主量元素采用X射线荧光光谱法(XRF)测试,分析精度2%,微量元素使用ICP-MS测试,分析精度5%。锆石颗粒的透射光、反射光、阴极发光照相及样品测年工作在中国地质调查局天津地质调查中心完成。U-Pb同位素测试使用仪器为LA-MC-ICPMS, ICP-MS型号为Agilent 7500a,激光束斑直径35 μm,频率为8 Hz,能量为5 mJ。分析时采用GJ-1作为年龄外标,NIST610作为元素含量外标;分析流程参见文献(Geng et al., 2017)。测试结果采用ICPMS DataCal(Liu et al.,

2010)程序进行数据处理,锆石U-Pb谐和图用Iso-plot3.0(Ludwig et al., 2000)程序绘制。

3 测试结果

锆石U-Pb测年结果见图3。锆石U-Pb年龄数据分属新太古代($2\ 663 \pm 22$ Ma~ $2\ 778 \pm 13$ Ma,样品D2053、D2079、D100)和古元古代($1\ 944 \pm 10$ Ma~ $2\ 006 \pm 10$ Ma,样品D081、D182、D5213)。

3.1 新太古代花岗质岩石

3件样品的锆石U-Pb年龄显示为新太古代,锆石多数并不完整,颜色为浅玫瑰红至深棕色,呈次圆状-长柱状,宽50~100 μm,长100~200 μm不等,多数锆石具有明显的岩浆环带结构,少部分具面状结构或核幔结构。样品D2053、D2079、D100三件样品的锆石存在不同程度的铅丢失,样品D100尤其明显,其 $^{206}\text{Pb}/^{238}\text{U}$ - $^{207}\text{Pb}/^{235}\text{U}$ 图显示(图4),不一致线与谐和线的上交点年龄为 $2\ 663 \pm 22$ Ma(MSWD =

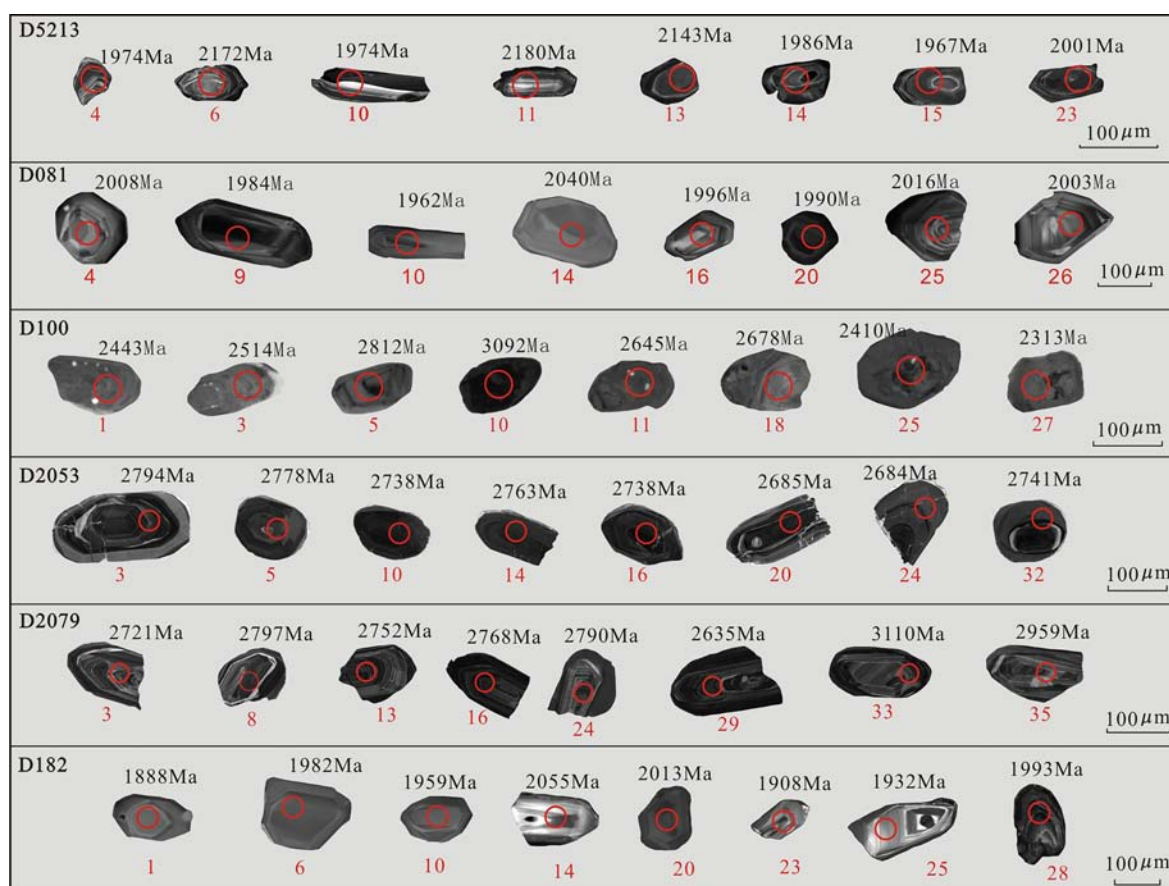


图3 坦桑尼亚卢帕地体锆石阴极发光图和年龄值

Fig.3 CL images and ages of the analyzed zircons in Lupa terrane, Tanzania

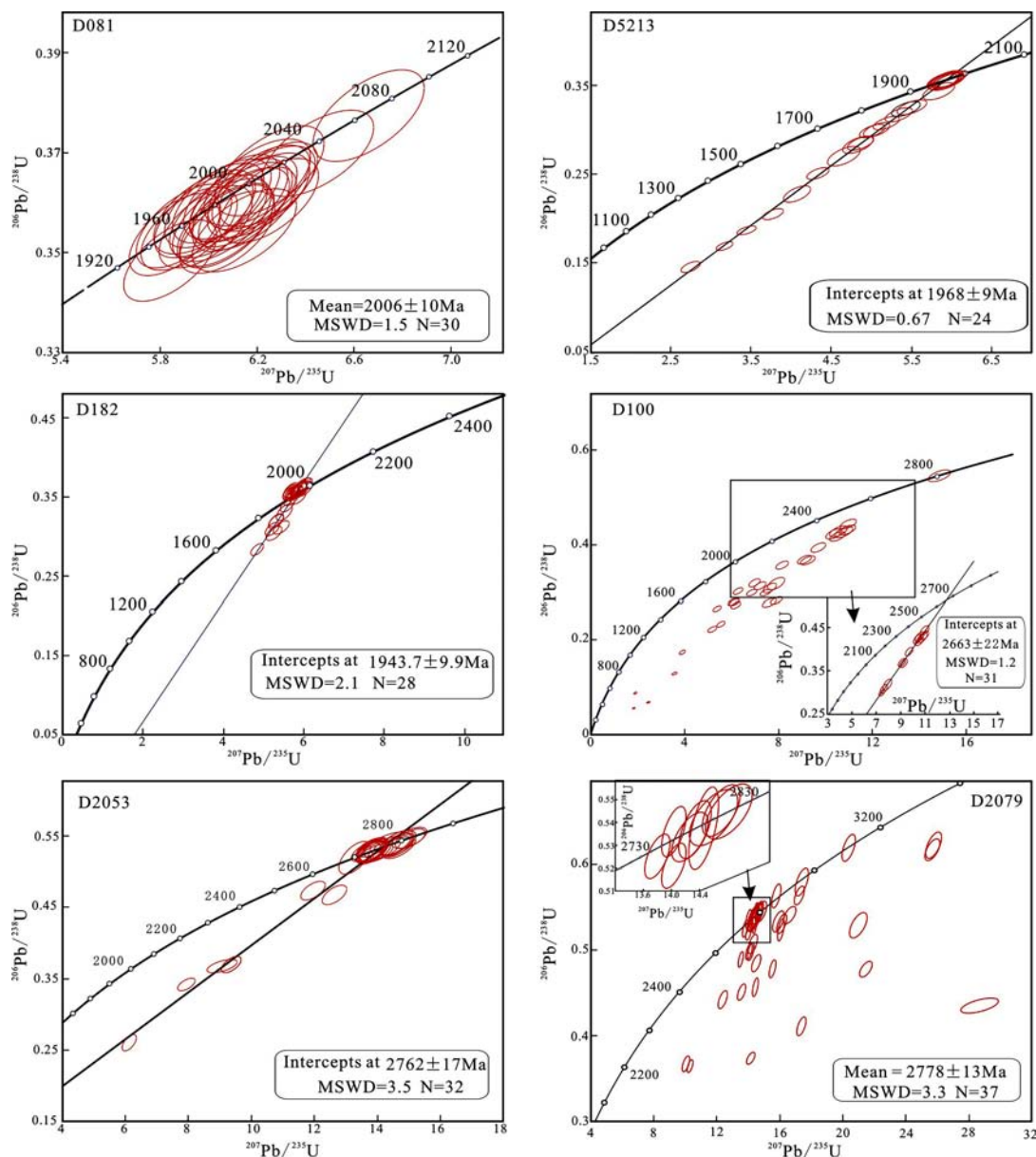


图4 坦桑尼亚卢帕地体锆石U-Pb谐和图

Fig.4 U-Pb concordia diagrams of Granitoids in Lupa terrane, Tanzania

1.2, N=31);样品D2053存在两组年龄,较新的一组可能代表成岩年龄,而较老的一组可能代表源区岩石年龄信息;其不一致线与谐和线的上交点年龄为 $2762 \pm 17\text{ Ma}$ (MSWD = 2.5, N=32),表明其原岩初始形成年龄为新太古代;样品D2079获得的锆石平均年龄为 $2778 \pm 13\text{ Ma}$ (MSWD = 3.3, N=37)。

新太古代花岗质岩石 SiO_2 的含量 $67.21\% \sim 77.80\%$, Al_2O_3 的含量 $12.21\% \sim 16.61\%$,全碱($\text{K}_2\text{O} + \text{Na}_2\text{O}$)的含量 $3.11\% \sim 7.96\%$, $\text{Na}_2\text{O}/\text{K}_2\text{O}$ 介于 $0.82 \sim 2.49$,仅样品D2079在深成岩TAS图(Wilson, 1989)

上落入花岗岩区域(图5)。 MgO 的含量介于 $0.16\% \sim 0.73\%$, $\text{Mg}\#$ 为 $10.45 \sim 38.35$,意味着其含有更多的地壳成分。 ΣREE 含量 $42.518 \times 10^{-6} \sim 79.112 \times 10^{-6}$, ΣLREE 值介于 $27.65 \times 10^{-6} \sim 74.36 \times 10^{-6}$, ΣHREE 值介于 $2.109 \times 10^{-6} \sim 4.752 \times 10^{-6}$, LREE/HREE 比值介于 $13.11 \sim 15.65$, $(\text{La}/\text{Yb})_N$ 值在 $22.8 \sim 32.7$ 之间,反映轻重稀土存在一定程度分异, δEu 值介于 $1.088 \sim 1.667$ 之间,显示Eu为正异常(图6)。

3.2 古元古代花岗质岩

古元古代锆石为无色至浅棕色,短柱-长柱状,

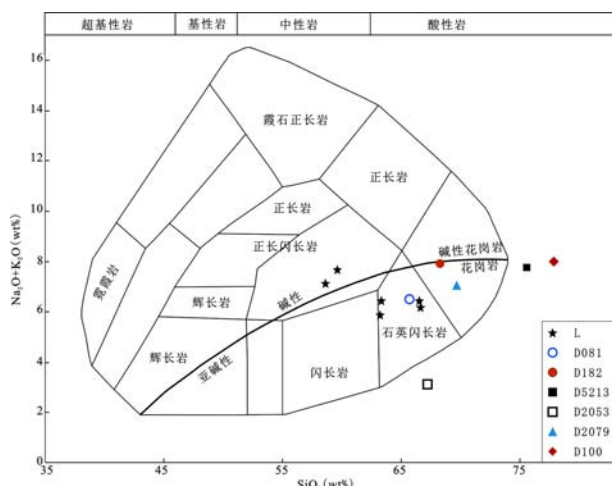


图5 卢帕地体酸性深成岩TAS图解(据Wilson, 1989)

Fig.5 TAS diagram of acid plutonite in Lupa terrane(after Wilson, 1989)

L—数据来源于(Manya, 2014);其他数据源自本文

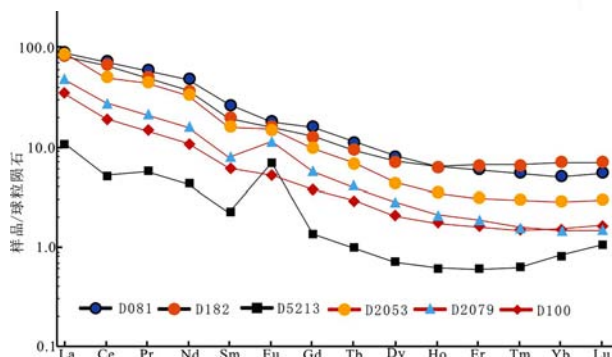


图6 卢帕地体球粒陨石标准化稀土配分图解

(球粒陨石标准化数值来源于文献

Sun and McDonough, 1989)

Fig.6 Chondrite normalized REE distribution diagram of Lupa terrane(the normalized value of chondrite was from Sun and McDonough, 1989)

宽30~80 μm,长50~150 μm,具明显的岩浆环带结构。样品D081、D182、D5213三件样品的锆石同样存在铅丢失情况,样品D081的 $^{206}\text{Pb}/^{238}\text{U}$ - $^{207}\text{Pb}/^{235}\text{U}$ 图指示的年龄数据为 $2\ 006 \pm 10\text{ Ma}$,与乌萨迦兰活动带的俯冲时间(Möller et al., 1995; Collin, et al., 2004)一致,样品D182、D5213的 $^{206}\text{Pb}/^{238}\text{U}$ - $^{207}\text{Pb}/^{235}\text{U}$ 图显示,其不一致线与谐和线的上交点为古元古代年龄数据 $1\ 944 \pm 10\text{ Ma}$, $1\ 967 \pm 9\text{ Ma}$ 。

采集的样品 SiO_2 的含量 $65.64\% \sim 77.8\%$, Al_2O_3 的含量结余 $12.21 \sim 16.61$,全碱($\text{K}_2\text{O} + \text{Na}_2\text{O}$)的含量 $6.49\% \sim 7.92\%$, $\text{Na}_2\text{O}/\text{K}_2\text{O}$ 介于 $0.94 \sim 5.36$,属富钠

铝质花岗岩类,样品D081在深成岩TAS图(Wilson, 1989)上落入花岗闪长岩区域,而样品D182落入花岗岩区域。 MgO 的含量介于 $0.21\% \sim 1.98\%$, $\text{Mg}\#$ 为 $37.45 \sim 48.26$,均高于太古宙花岗质岩石(MgO 含量 $0.16\% \sim 0.73\%$, $\text{Mg}\#$ 为 $10.45 \sim 38.35$),古元古代花岗质岩石可能比太古宙花岗质岩石具有更多的地幔来源,或混入了部分熔融的下地壳玄武质岩石。

样品D5213的 ΣREE 含量为 9.875×10^{-6} ,LREE含量为9.060,HREE含量为0.815, $(\text{La}/\text{Yb})_{\text{N}}=13.1$, $\delta\text{Eu}=3.848$,具Eu正异常(图6),其轻重稀土轻微分异。而样品D100、D081的 ΣREE 分别为 94.260×10^{-6} 、 106.870×10^{-6} , ΣLREE 含量分别为 86.480×10^{-6} 和 98.640×10^{-6} , ΣHREE 含量分别为 7.780×10^{-6} 和 8.230×10^{-6} , $(\text{La}/\text{Yb})_{\text{N}}$ 值分别为11.8、17.6, δEu 值分为0.979、0.841,具Eu弱负异常(图6),其轻重稀土轻微分异,样品D5213的物质来源、成因与样品D100、D081可能不同,其可能有更多的地幔来源。

4 讨论

4.1 形成时代

本文报告的卢帕地体中的花岗岩类锆石U-Pb年龄指示了其分属新太古代($2\ 663 \pm 22\text{ Ma} \sim 2\ 778 \pm 13\text{ Ma}$)和古元古代($1\ 944 \pm 10\text{ Ma} \sim 2\ 006 \pm 10\text{ Ma}$),二者的锆石有不同程度的铅丢失情况,说明其受后期的构造-热事件影响较大,并且太古宙的锆石铅丢失更严重(图4)。伊伦加山附近的花岗岩类锆石U-Pb年龄也具有相似的组成(Lawley et al., 2013a),太古宙锆石U-Pb年龄($2\ 723 \pm 10\text{ Ma} \sim 2\ 758 \pm 9\text{ Ma}$)则与本文报道时间基本一致,但是古元古代的锆石U-Pb年龄可进一步分为 $1\ 935 \pm 1\text{ Ma} \sim 1\ 960 \pm 1\text{ Ma}$ 和 $1\ 880 \pm 17\text{ Ma} \sim 1\ 891 \pm 17\text{ Ma}$ 两组,前者与本文报道的古元古代锆石U-Pb年龄基本一致,后者为卢帕金矿田金成矿年龄(Lawley et al., 2013a)。此外,前人工作报道的萨扎(Saza)辉长岩的锆石U-Pb年龄为 $1\ 758 \pm 33\text{ Ma}$ (Manya, 2012),Nasmyia基性-超基性岩的锆石U-Pb年龄介于 $1\ 874 \sim 1\ 944\text{ Ma}$ (吴兴源等,2018),这都说明卢帕地体的岩浆事件集中发生于新太古代-古元古代。卢帕地体西北部的Ngulla碳酸岩($1\ 040 \pm 40\text{ Ma}$)(Cahen and Snelling, 1966),

可能代表了新元古宙的一次裂谷作用,暗示了罗迪尼亞超大陸裂解开始的时间(Cahen and Snelling, 1966, 孙凯等, 2022)。

4.2 物质来源

样品D5213、D081、D5213、D2079、D100的A/CNK值介于1.01~1.12,暗示为I型花岗岩,而样品D182和D2053的A/CNK值分别为0.997和0.867,为铝不饱和的碱性花岗岩(肖庆辉, 2002; 郑永飞等, 2013),说明花岗岩的物质来源主要为地壳内部岩浆岩。

图7a-7d(Collins et al., 1982; Whalen et al., 1987)显示,太古宙花岗岩和古元古代花岗岩均为非A型花岗岩,其物质来源并非来自地幔,而是地壳重熔的结果。卢帕地体内萨扎地区的太古宙花岗岩类(花岗闪长岩)被认为是与太古宙长英质地壳有关的岩浆混合形成(Manya, 2011; Lawley et al., 2013a),而该地区的基性超基性岩则被认为部分熔融的地幔岩浆混入了太古宙地壳(Manya, 2014)。区域上古元古代Nasmyth基性-超基性岩被认为来源于

古元古代俯冲作用下的岩石圈地幔与下地壳基底混染形成(许康康等, 2021),而Ngulla地区的玄武质安山岩和斑状英安岩的 ϵ_{Nd} 值介于-3.33~-6.24,其原岩被认为来源于地壳物质的重熔(Tulibonywa et al., 2015)。

4.3 构造环境

在花岗岩Hf-Rb-Ta*3判别图解(图8a)(杨学明等, 2000)显示,所有的样品都投影在火山弧花岗岩中,而Rb-(Yb+Ta)判别图解中(图8b)(Pearce et al., 1984)仅D182、D2053、D081三件样品落在判别图解的火山弧花岗岩中,而样品D2079、D5213、D100投影在判别图解之外。花岗岩K₂O-SiO₂判别图解(图8c)(Coleman and Peterman, 1975)和花岗岩Rb-Sr判别图解(图8d)(Coleman and Peterman, 1975)中,样品投影均远离大洋花岗岩、大洋玄武岩和辉长岩区域,集中于大陆花岗岩区域,表明花岗岩形成的构造环境为大陆边缘弧环境,这与卢帕地体内萨扎地区的太古宙花岗岩的构造环境一致(Lawley et al., 2013a; Tulibonywa et al., 2015)。卢

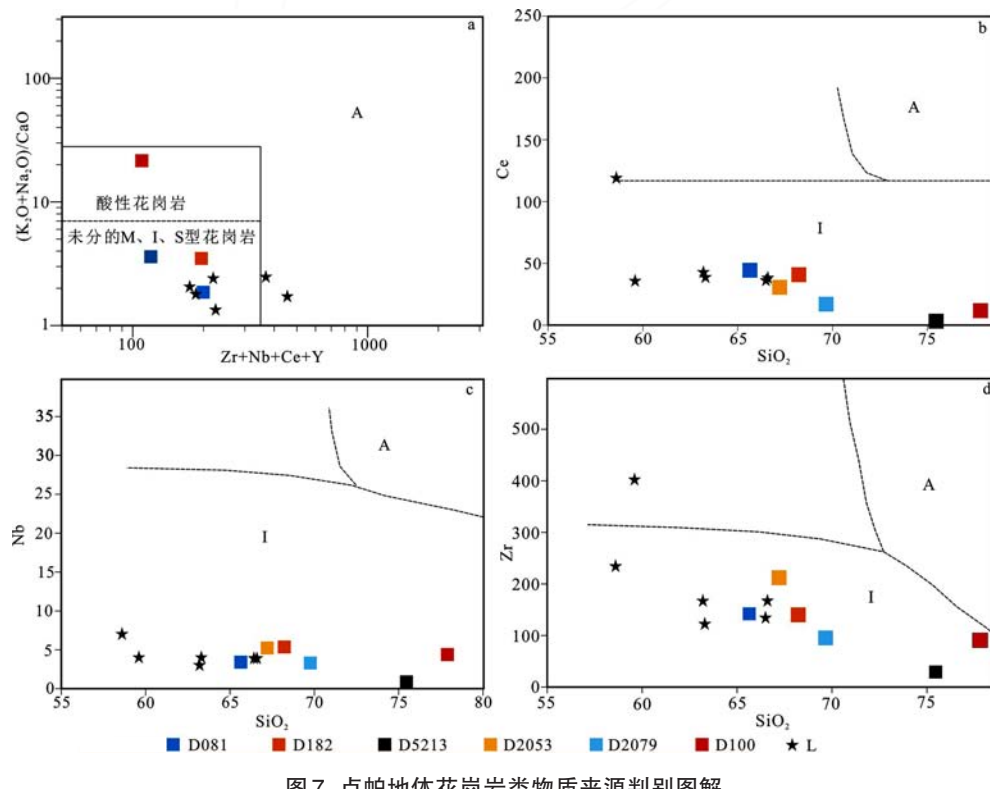


图7 卢帕地体花岗岩类物质来源判别图解

Fig.7 Discrimination diagrams of granitoids in Lupa terrane

a. $(\text{Zr}+\text{Nb}+\text{Ce}+\text{Y}) - [(\text{K}_2\text{O}+\text{Na}_2\text{O})/\text{CaO}]$; b. $\text{SiO}_2 - \text{Ce}$; c. $\text{SiO}_2 - \text{Ga}$; d. $\text{SiO}_2 - \text{Zr}$;

L. 数据来源于(Manya, 2014);其他数据源自本文(a.据Whalen et al., 1987; b/c/d.据Collins et al. 1982)

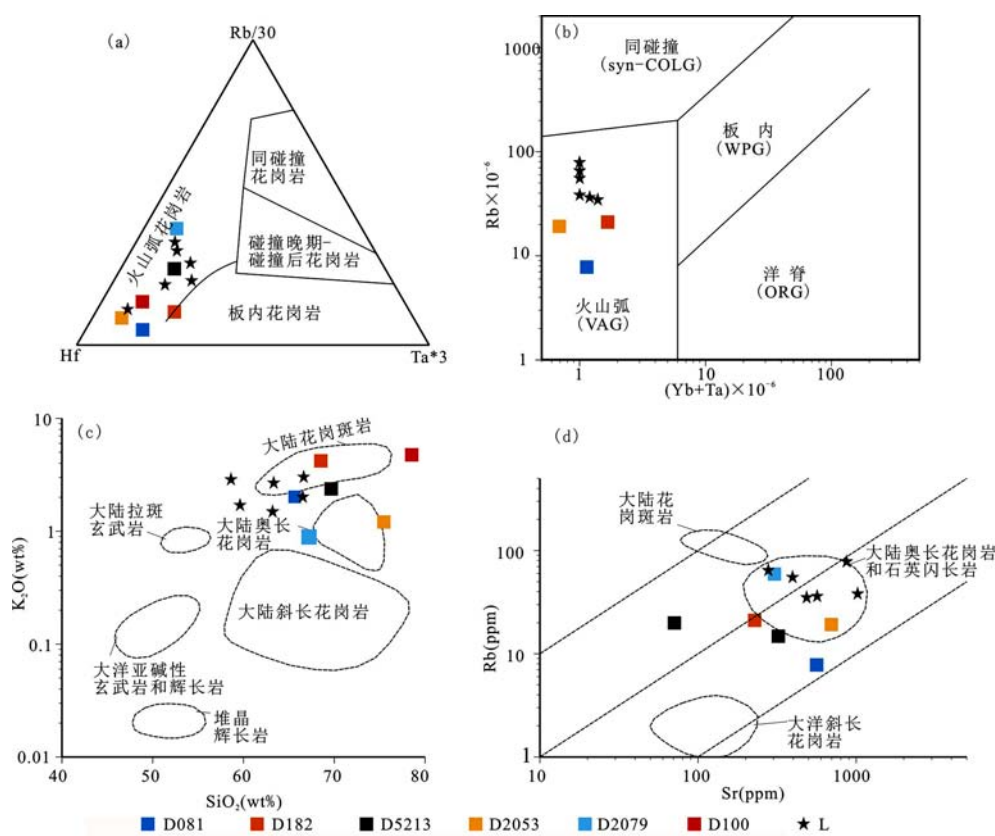


图8 卢帕地体花岗岩类构造环境判别图解

Fig.8 Identification diagram of tectonic setting in Lupa terrane

a. Hf-Rb-Ta*3; b. Rb-(Yb+Ta); c. K₂O-SiO₂; d. Rb-Sr; L. 数据来源于(Manya, 2014);

其他数据源自本文(a. 据杨学明等, 2000; b. 据Pearce et al., 1984; c/d. 据Coleman and Peterman, 1975)

帕地体呈正地形, 相对高差最高可达1 500 m, 高海拔地区紧邻鲁夸断裂带, 代表大陆边缘弧环境(Manya 2014; Lawley et al., 2013a), 暗示洋陆俯冲作用发生于卢帕地体以西(Manya, 2014)。

卢帕地体西北的卡通马地体(Katuma terrane)经历了时代为2.65 Ga、2.05 Ga、1.97 Ga和1.88 Ga的4次变质事件(Kazimoto et al., 2014), 与卢帕地体的构造-岩浆-热事件的时间相吻合, 暗示卢帕地体同样在太古宙地壳形成后, 经历了至少3次构造-热事件, 最终形成当前构造的基本格局。与2.05 Ga和1.88 Ga同时代的榴辉岩已分别在乌萨迦兰带和乌本迪带内发现(Möller et al., 1995; Collins et al., 2004; Boniface et al., 2012), 说明同期卢帕地体和卡通马地体发生的构造-热事件为对洋壳俯冲作用的响应。卢帕地体内部和其北部大规模出露的古元古代花岗岩(Manya, 2011, 2014; Boniface and Schenk, 2012; Boniface et al., 2012; Lawley et al., 2013a), 证

明其在洋壳俯冲作用发生时期, 古老地壳普遍经历了重熔作用, 而卢帕地体内的太古宙花岗岩应为重熔的残留体, 推测卢帕地体北部至伦瓜镇地区为弧后盆地构造环境。

5 结论

卢帕地体主要由岩浆岩组成, 以花岗岩类为主。花岗岩的主要形成年龄为古元古代($1\ 944 \pm 10$ Ma~ $2\ 006 \pm 10$ Ma), 部分地区残留太古宙岩石($2\ 663 \pm 22$ Ma~ $2\ 778 \pm 13$ Ma)。花岗岩的岩石地球化学特征表明非A型花岗岩, 其物质来源并非来自地幔, 而是地壳重熔的结果。花岗岩构造环境判别图解显示新太古代与古元古代的花岗岩形成于大陆边缘弧。

致谢:感谢坦桑尼亚地质调查局A. H. Mruma教授对本项目野外工作的大力支持。感谢坦桑尼亚地质调查局Elisa Mphuru工程师在野外地质工作中给

于的帮助。同时,衷心感谢审稿人提出的宝贵修改意见和建议。

中文参考文献

- 龚鹏辉,刘晓阳,孙凯,等.2023.浅析坦桑尼亚卡鲁超群地质特征及含矿性[J].华北地质,46(1):50-60.
- 何胜飞,刘晓阳,孙凯,等.2021.坦桑尼亚古元古代姆柏兹地体锆石U-Pb-Hf同位素特征及其指示的构造环境研究[J].地质学报,95(4),976-998.
- 李生喜,何碧,杨博,等.2023.南天山地块塔格拉克地区二长花岗岩锆石U-Pb年代学、地球化学特征:对壳源岩浆成因和构造背景的限定[J].中国地质,50(2):622-639.
- 刘晓阳,龚鹏辉,许康康,等.2020.坦桑尼亚乌本迪活动带西北部元古宙沉积盆地碎屑锆石U-Pb年龄及其地质意义[J].地质调查与研究,43(1):5-18.
- 孙凯,张航,卢宜冠,等.2022.中非铜钴成矿带地质特征与找矿前景分析[J].中国地质,49(1):103-120.
- 王杰,刘晓阳,任军平,等.2022.坦桑尼亚前寒武纪成矿作用[J].华北地质,45(1):101-110.
- 吴兴源,刘晓阳,王杰,等.2018.坦桑尼亚乌本迪造山带的演化、金成矿作用研究进展及中国—坦桑尼亚造山型金矿床的异同[J].地质论评,64(01):165-182.
- 肖庆辉.2002.花岗岩研究思维与方法[M].北京:地质出版社,1-294.
- 许康康,刘晓阳,孙凯,等.2021.坦桑尼亚西南部乌本迪带内Nsanya镁铁-超镁铁质杂岩体的锆石U-Pb年龄、地球化学特征及构造意义[J].地质学报,95(4):1174-1190.
- 许康康,刘晓阳,孙凯,等.2020.坦桑尼亚乌本迪带内花岗岩类的LA-MC-ICP-MS锆石U-Pb年龄及地质意义[J].地质调查与研究,43(1):55-71.
- 许康康,刘晓阳,赵晓博,等.2024.坦桑尼亚乌本迪带内基性-酸性岩类的锆石U-Pb年龄、地球化学特征及地质意义[J].西北地质,57(3):210-223.
- 许康康,刘晓阳,王杰,等.2019.坦桑尼亚西南部乌本迪带的构造演化特征[J].地质与勘探,55(02):585-599.
- 杨学明,杨晓勇,陈双喜.2000.岩石地球化学[M].合肥:中国科学技术大学出版社,1-275.
- 曾国平,王建雄,向文帅,等.2024.厄立特里亚西部新元古代岛弧花岗岩对东非造山带构造演化的指示意义[J].西北地质,57(2):159-173.
- 郑永飞,杨进辉,宋述光,等.2013.化学地球动力学研究进展[J].矿物岩石地球化学通报,32(1):1-24.

References

- Boniface N, Appel P. 2018. Neoproterozoic reworking of the Ubendian Belt crust: Implication for an orogenic cycle between the Tanzania Craton and Bangweulu Block during the assembly of Gondwana [J]. Precambrian Research, 305, 358-385.
- Boniface N, Schenk V, Appel P. 2012. Paleoproterozoic eclogites of MORB-type chemistry and three Proterozoic orogenic cycles in the Ubendian Belt (Tanzania): Evidence from monazite and zircon geochronology, and geochemistry [J]. Precambrian Research, 192-195:16-33.
- Boniface N, Schenk V., Appel P. 2014. Mesoproterozoic high-grade metamorphism in pelitic rocks of the northwestern Ubendian Belt: Implication for the extension of the Kibaran intra-continental basins to Tanzania [J]. Precambrian Research, 249: 215-228.
- Boniface N, Schenk V. 2012. Neoproterozoic eclogites in the Paleoproterozoic Ubendian Belt of Tanzania: Evidence for a Pan-African suture between the Bangweulu Block and the Tanzania Craton [J]. Precambrian Research, 208-211: 72-89.
- Cahen L, Snelling N J. 1966. The Geochronology of Equatorial Africa[M]. North Holland, Amsterdam, 1-195.
- Coleman R G, Peterman Z E. 1975. Oceanic plagiogranite[J]. Journal of Geophysical Research, 80(8):1099-1108.
- Collins W, Beams S, White A, et al. 1982. Nature and Origin of A-type granites with particular reference to southeastern Australia[J]. Contributions to Mineralogy and Petrology, 80(2): 189 - 200.
- Collins A S, Reddy S M, Buchan C, Mruma A. 2004. Temporal constraints on Palaeoproterozoic eclogite formation and exhumation (Usagaran Orogen, Tanzania) [J]. Earth and Planetary Science Letters 224 (1 - 2), 175-192.
- Daly M C, Klerkx J, Nanyaro J T. 1985. Early Proterozoic terranes and strike-slip accretion in the Ubendian Belt of southwest Tanzania [J]. Terra Cognita, 5: 257.
- Daly M C. 1988. Crustal shear zones in central Africa: a kinematic approach to Proterozoic tectonics [J]. Episodes, 11: 5-11.
- Geng J Z, Qiu K F, Gou Z Y, et al. 2017. Tectonic regime switchover of Triassic Western Qinling Orogen: Constraints from LA-ICP-MS zircon U - Pb geochronology and Lu - Hf isotope of Dangchuan intrusive complex in Gansu, China [J]. Geochemistry, 77: 637 - 651.
- Guest N J. 1954. Petrographical notes on some rocks outcropping near the road from Chunya to Itigi [J]. Records of the geological survey of Tanganyika, IV, 105 - 109.
- Kazimoto E O, Schenk V, Berndt J. 2014. Neoarchean and Paleoproterozoic crust formation in the Ubendian Belt of Tanzania: Insights from zircon geochronology and geochemistry [J]. Precambrian Research, 252: 119 - 144.
- Lawley C J M, Selby D, Condon D J, et al. 2013a. Lithogeochronology, geochronology and geodynamic setting of the Lupa Terrane, Tanzania: implications for the extent of the Archean Tanzanian Craton [J]. Precambrian Research, 231: 174 - 193.
- Lawley C J M., Selby D., Condon D., et al. 2014. Palaeoproterozoic orogenic gold style mineralization at the Southwestern Archaean Tanzanian cratonic margin, Lupa Goldfield, SW Tanzania: Implications from U-Pb titanite geochronology [J]. Gondwana Research, 26(3-4), 1141 - 1158.
- Lawley C, Selby D, Imber J. 2013b. Re-Os Molybdenite, Pyrite, and Chalcopyrite Geochronology, Lupa Goldfield, Southwestern Tanzania: Tracing Metallogenetic Time Scales at Midcrustal Shear Zones Hosting Orogenic Au Deposits [J]. Economic geology and the bulletin of the Society of Economic Geologists, 108(7), 1591 - 1613.

(下转至本期第35页)

- 用[J].东华理工大学学报:自然科学版,40(1):42-46.
- 吴曲波,黄伟传,乔宝平,等.2020.砂岩型铀矿三维地震勘探采集关键技术及效果[J].地球物理学进展,35(6):2239-2249.
- 辛思华,宋仁成,杨建军.2008.高密度电法在煤矿采空区勘查中的应用[J].中国煤炭地质,20(1):59-61.
- 杨玉蕊,张义平,缪玉松,等.2012.高密度电法中勘探线长度与测深关系浅析[J].中国煤炭地质,24(6):63-68.
- 叶发旺,张川,李瀚波,等.2021.“空天”高分辨率遥感技术及其在铀资源勘查中的应用进展与发展建议[J].铀矿地质,37(3):313-329.
- 俞初安,金若时,李彤,等.2023.鄂尔多斯盆地砂岩型铀矿成矿地质条件和关键控矿要素分析[J].地球学报,44(4):689-706.
- 俞初安,司马献章,李建国,等.2018.鄂尔多斯盆地直罗组地层岩性测井响应特征[J].煤田地质与勘探,46(6):33-41.
- 俞初安,孙大鹏,周小希,等.2022.基于自然伽马测井数据的铀资源评价方法研究—以鄂尔多斯盆地彭阳铀矿区为例[J].煤田地质与勘探,50(5):144-153.
- 俞初安,吴兆剑,司马献章,等.2020.二连盆地马尼特坳陷南缘赛汉组砂岩碎屑锆石年龄及其地质意义[J].地球科学,45(5):1609-1621.
- 张必敏,王学求,徐善法,等.2020.穿透性地球化学勘查技术在隐伏砂岩型铀矿调查中的应用研究[J].地球学报,41(6):770-784.
- 赵宁博,付锦,刘涛,等.2017.地形对砂岩型铀矿氡气测量的干扰作用及其修正方法[J].物探与化探,41(4):667-671.
- 赵希刚,张云宜,赵翠萍,等.2010.砂岩型铀矿找矿中物化探测量方法应用评述及建议[J].世界核地质科学,27(1):31-37.

References

Ellit J R. 1968. Magnetic susceptibility and geochemical relationships

- as uraumn prospecting duides[J].USAEC.AEC-RI, 53-56.
- Gray T, Kinnaird J, Laberge J, et al. 2021.Uraniferous leucogranites in the Rössing area, Namibia: New insights from geologic mapping and airborne hyperspectral imagery[J]. Economic Geology, 116 (6): 1409-1434.
- Hou Baohong, Keeling John , Li Ziying. 2017. Paleovalley-related uranium deposits in Australia and China: A review of geological and exploration models and methods[J].Ore Geology Reviews, 88: 201-234.
- LEBEL D. 2020. Geological Survey of Canada 8.0: Mapping the journey towards predictive geoscience [J]. Geological Society, London, Special Publications, 499(1):49-68.
- Michael J, Michael Z. 2019. Imaging Yellowstone magmatic system by the joint Gramian inversion of gravity and magnetotelluric data[J].Physics of the Earth and Planetary Interiors, 292:12-20.
- Nie Fengjun, Yan Zhaobin, Feng Zhibing, et al. 2020. Genetic models and exploration implication of the paleochannel sandstone-type uranium deposits in the Erlian Basin, North China-A review and comparative study[J]. Ore Geology Reviews, 127,1-36.
- Jin Ruoshi, Miao Peisen, Sima Xian-zhang, et al. 2018. New prospecting progress using information and big data of coal and oil exploration holes on sandstone-type uranium deposit in North China[J]. China Geology, 167-168.
- R. Penney, C. Ames, D. Quinn and A. Ross. 2017. Determining uranium concentration in boreholes using wireline logging techniques: comparison of gamma logging with prompt fission neutron technology (PFN) [J]. Applied Earth Science, 121:2, 89-95.

(上接本期第 22 页)

- Leger C, Barth A, Falk D, et al. 2015. Explanatory notes for the mineralogic map of Tanzania [M]. Dodoma: Geological Survey of Tanzania. 1-376.
- Lenoir J L, Liegeois J P, Theunissen K et al. 1994. The Palaeoproterozoic Ubendian shear Belt in Tanzania: geochronology and structure [J]. Journal of African Earth Sciences, 19: 169-184.
- Liu Y S, Hu Z C, Zong K Q, et al. 2010. Reappraisal and refinement of zircon U-Pb isotope and trace element analyses by LA-ICP-MS [J]. Chinese Science Bulletin, 55(15): 1535-1546.
- Ludwig K R. 2000. User's Manual for Isoplot/Ex Version 2.2: A Geochronological Toolkit for Microsoft Excel. Berkeley Geochronology Center [J]. Special Publication, 1: 1-50.
- Manya S. 2012. SHRIMP zircon U-Pb dating of the mafic and felsic intrusive rocks of the Saza area in the Lupa goldfields, southwestern Tanzania: Implication for gold mineralization [J]. Natural Science, 04(09): 724-730.
- Manya S. 2014. Geochemistry of the Palaeoproterozoic gabbros and granodiorites of the Saza area in the Lupa Goldfield, southwestern Tanzania [J]. Journal of African Earth Sciences, 100: 401-408.
- Manya S. 2011. Nd-isotopic mapping of the Archaean - Proterozoic boundary in southwestern Tanzania: Implication for the size of the

Archaean Tanzania Craton [J]. Gondwana Research, 20(2-3), 325-334.

- MÖller, A., Appel, P., Mezger, K., Schenk, V., 1995. Evidence for a 2 Ga subduction zone: eclogites in the Usagaran Belt of Tanzania [J]. Geology 23 (12), 1067-1070.
- Pearce J A, Harris N B, Tindle A G. 1984.Trace element discrimination diagrams for the tectonic interpretation of granitic rocks[J]. Journal of Petrology, 25: 956-983.
- Sun S S, McDonough W F. 1989.Chemical and isotope systematics of oceanic basalts: Implications for mantle composition and processes. In: Saunders A D, ed. Magmatism in Ocean Basins[C]. Spec Publ Geol Soc Lond, 42: 313-345.
- Tulibonywa T, Manya S, Maboko M A H. 2015.Palaeoproterozoic volcanism and granitic magmatism in the Ngwalla area of the Ubendian Belt, SW Tanzania: Constraints from SHRIMP U-Pb zircon ages, and Sm-Nd isotope systematics [J]. Precambrian Research, 256: 120-130.
- Whalen J B, Currie K L, Chappell B W. 1987.A-type granites: geochemical characteristics, discrimination and petrogenesis[J]. Contributions to Mineralogy and petrology, 95(4): 407 - 419.
- Wilson M. 1989.Igneous Petrogenesis [M]. Chapman and hall, London, 1-466.